

Chapter 3

Fermilab E769

During the 1986-87 fixed target run at Fermi National Accelerator Laboratory (Fermilab), approximately 400 million events were written to tape by the collaborators of Experiment #769 (E769). E769, an experiment designed to study the hadroproduction of charm (with a variety of beams and target materials), inherited the Tagged Photon Lab (TPL) spectrometer from its predecessor E691, whose purpose had been to study charm photoproduction. After the completion of E769 data taking, the TPL spectrometer was again put to use, this time by E791, a successor hadroproduction experiment which used a π^- beam to obtain an extremely large data set well-suited to high-statistics studies of charm production and decay. The TPL spectrometer, located at the end of the Proton East secondary beam line, underwent various changes and modifications through the years. In Fig. 3.1, a diagram of the detector as used by E769 is given. In this chapter we describe E769's mixed hadron beams, multifoil target, and various components of the TPL spectrometer, emphasizing those which are used in this analysis. Detailed descriptions of the experiment components can be found in the references cited in [6] and in references cited below for specific spectrometer components.

My personal involvement with E769 began in the spring of 1992, when I joined the collaboration with Prof. Paul Karchin as my thesis advisor. By that time, the experimental running and off-line event reconstruction had been completed. My contribution to the research effort therefore consisted of data analysis; one of my first

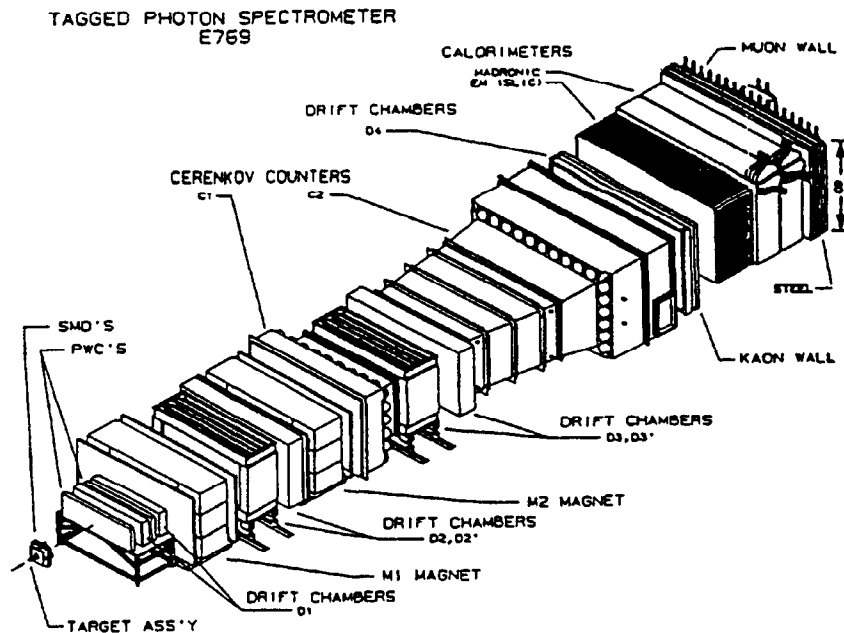


Figure 3.1: Tagged Photon Lab spectrometer.

tasks was to modify the program used to reconstruct Monte Carlo events (Chapter 4) to include a simulation of the two-stage reconstruction used for the data.¹ The remainder of my time at Yale was spent executing the various stages of analysis (beginning at the substrip level) described in this thesis, the product of which are the measurements presented herein.

3.1 Beams

E769 uses secondary mixed hadron (π , K , p (\bar{p})) beams obtained by extracting protons from the Tevatron's 800 GeV beam, directing them into a Be target, and intercepting the products of the ensuing inelastic collisions. A dipole magnet is used to select the desired charge sign and momentum of the secondary beam; these particles are

¹The second stage was necessary due to errors in the first attempt at event reconstruction (see Section 5.1).

collimated, focussed, and sent down the various fixed-target beam lines. Time scales characterizing the beam are determined by the acceleration and extraction processes. The radio-frequency electromagnetic field used to accelerate protons in the Tevatron confines beam particles in “buckets” of 1 ns duration coming every 19 ns. Extraction of protons from the Tevatron takes place in “spills” of 22 second duration every 60 seconds. Secondary beam particles reaching TPL are relatively isolated in time; on average only about one in 50 buckets is occupied.

In the first half of the experiment, the sign of the beam particles’ charge was selected to be negative; this polarity was reversed to positive for the remainder of the running. Except for a period during which roughly 15% of the negative beam data was taken at 210 GeV, the beam momentum was kept at 250 GeV, corresponding to a hadronic center-of-mass energy of 21.7 GeV. The negative beam consists on average of 93% π^- , 5% K^- , and 1.5% \bar{p} , the positive of 61% π^+ , 4.4% K^+ , and 34% p ; these percentages are known as *a priori* beam particle probabilities.²

Upstream of the target, eight proportional wire chamber (PWC) planes and two silicon microstrip detector (SMD) planes³ allow for beam tracking, a capability which is not used in this analysis. As mentioned in Section 3.2, however, beam PWC hit information is used to facilitate beam particle identification in the positive running.

3.2 Beam particle identification

For purposes of this analysis, a beam particle is defined as positively identified if the calculated probability that its tag is correct is at least 90%. Two pieces of E769 apparatus are dedicated to the event-by-event identification of the three hadronic species in the beam: a differential isochronous self-focussing Čerenkov counter (DISC) and a transition radiation detector (TRD).⁴

The DISC operates through the detection of Čerenkov light emitted at a fixed

²These *a priori* probabilities are measured using DISC information (see Section 3.2).

³See Sections 3.4.2 and 3.4.1 for a description of PWC and SMD operation, respectively.

⁴The DISC and TRD are situated in the beam line upstream of the target assembly and are therefore not depicted in Fig. 3.1. Detailed descriptions of the DISC and TRD can be found in [20] and [25], respectively.

angle (24.5 mrad) with respect to the beam axis. Čerenkov radiation occurs when the speed of a charged particle in a medium exceeds the speed of light in that medium; the angle $\theta_{\check{C}}(B)$ at which beam particle B emits Čerenkov light is given by

$$\theta_{\check{C}}(B) = \frac{1}{n \beta(B)} = \frac{1}{n \sqrt{1 + (m(B)/P_{beam})^2}}, \quad (3.1)$$

where $\beta(B)$ is B 's speed normalized to the speed of light (in vacuum) and n is the index of refraction of the medium through which the particle passes, which in the case of the DISC is He gas. The velocities of the three hadron species are determined by the common momentum P_{beam} and their masses $m(B)$. The DISC is “set” to identify one of the three by tuning n , which for a gas increases with density. By adjusting the pressure of the He gas (given the current ambient temperature), a value of n is achieved such that $\theta_{\check{C}}(B)$ equals the angle at which reflected and focussed Čerenkov light passes through an annular slit and onto an array of eight photomultiplier tubes (PMTs), two in each quadrant of the transverse plane. Identification of a beam particle to which the DISC is set requires four or more coincident PMT hits, at least one in each transverse quadrant.⁵

The TRD is made up of 24 identical modules sitting in the beam line, each consisting of a transition radiator (TR) followed by a pair of PWC planes. Each TR is a set of eight polypropylene foils separated by gaps filled with He gas. Relativistic charged particles, upon traversing these alternating media, induce local time-dependent polarizations which radiate in a forward cone; the intensity of this radiation is proportional to $\gamma(B)$, where

$$\gamma(B) \equiv \frac{1}{\sqrt{1 - \beta^2(B)}} = \sqrt{1 + (P_{beam}/m(B))^2}, \quad (3.2)$$

thus enabling discrimination of beam particle species on the basis of mass. The PWCs are filled with a gas mixture (90% Xe, 10% methylal) which renders them more

⁵By plotting the number of positive DISC hits per unit beam flux as a function of He pressure, we obtain a “pressure curve”, in which π , K , and p peaks are evident. Pressure curves were taken periodically during the experimental running; the relative areas of the three peaks provide a measure of the *a priori* beam particle probabilities.

sensitive to X-ray photons than to relativistic bremsstrahlung. The modules are designed so that, at E769's beam momentum of 250 GeV, detection of a photon in a given PWC plane is probable only for pions. Combining the outputs of the 48 PWCs allows for good separation in the response of the TRD to pions and non-pions. Identification of a beam particle as a pion requires that the number of TRD plane hits exceed a minimum cutoff (~ 12), which is calibrated periodically as running conditions change.

The \bar{p} component of the negative beam is negligible. During the negative running, therefore, information from the DISC (set to tag kaons) alone is used in beam particle identification. In the positive running, where discrimination between three species is required, a two-step process using both the DISC and TRD is implemented. First, the output of the DISC (set to either kaons or protons) is examined. If positive identification results, the process ends. Otherwise, TRD output is used to separate pions from non-pions.⁶ If the DISC is set to tag kaons, the absence of a DISC tag leads to positive identification of non-pions as protons.

The average efficiency of beam particle identification depends upon the species, the means by which it is identified, and the level of contamination tolerated in a B sample considered positively identified. Identification by DISC has an efficiency of roughly 40%, independent of B . TRD identification is even more efficient (80-90%, not including the PWC cluster cut efficiency). In all cases, the performance of E769's beam particle identification system exceeded the 90% correct-tagging standard used to define B samples; beam contaminations significantly lower than 10% are realized, as listed in Table 3.1.

In the vicinity of the TRD are two scintillators used in the event logic (see Sections 3.5 and 3.6) to signal the presence of incident beam particles.

⁶Accurate interpretation of the number of TRD plane hits relies upon the presence of only one beam particle per bucket; this is insured by requiring that the number of hit clusters found in the beam PWCs not exceed the number of planes. The average efficiency of this cut is measured to be 81%.

Beam	π	K	p, \bar{p}
π^-	-	3.8%	1.5%
K^-	1.0%	-	0.0%
π^+	-	0.0%	0.6%
K^+	0.1%	-	0.0%
p	0.3%	4.8%	-

Table 3.1: Beam contaminations.

3.3 Target

The E769 multifoil target is designed to allow study of the dependence of charm production on the atomic mass A of the nuclear target. A total of 26 foils (14 Be, 5 Al, 3 Cu, and 4 W), comprising approximately 2% of a nuclear interaction length, provide data points ranging over an order-of-magnitude in A . As discussed in Section 5.4, the widths of the foils ($\sim 100 \mu$ for W, $\sim 250 \mu$ for Be, Al, and Cu) enable more precise determination (in z) of charm production point positions than allowed by the vertex resolution achieved through SMD tracking (see Section 3.4.1).

Immediately upstream of the target foils are two scintillators, the beam spot and halo counters; downstream of the target foils is the interaction scintillator. The output of these three scintillators is used in the trigger logic (see Section 3.5) to signal the occurrence of interactions within the target. In addition, the interaction scintillator is considered in this analysis an additional target component, for a total target thickness of 2.5% nuclear interaction lengths. In Table 3.2, characteristics of these components relevant to cross-section or beam attenuation calculations are compiled.

In this analysis, linear dependence of charm production on A is assumed;⁷ we therefore need only characterize the target in terms of its total “nucleonic thickness” (i.e., nucleons per unit cross-sectional area). In order to calculate attenuation of the beam upstream of and within the target, the thicknesses of each material must be

⁷See discussion in Section 8.1.

Material	total thickness (cm)	total nuclear interaction lengths (%)	density (g/cm ³)
Be	0.3629	0.892	1.848
Al	0.1261	0.320	2.70
Cu	0.0761	0.504	8.96
W	0.0383	0.399	19.3
int. scint. ^a	0.3175	0.395	1.02

^aThe interaction scintillator is made of polyvinyltoluene, characterized by a H/C ratio of ~ 1.1 .

Table 3.2: Target component characteristics.

expressed in terms of nuclear interaction lengths, which are derived from nuclear inelastic cross-sections (σ_I); these cross-sections, in addition to depending on the beam particle species,⁸ exhibit A -dependence of the form $A^{0.71}$. As defined in Section 8.1, the formula for effective beam particle flux (as “seen” by a process linear in A) must therefore incorporate the attenuation factors χ_{att} , equal to 98.2% (98.8%) for proton (meson) beam(s).

The (right-handed) coordinate system with which we define the spectrometer has its origin on the beam line immediately downstream of the interaction scintillator. The z -axis is the beam line; z is positive downstream of the origin. The y -axis points upward (towards the roof of TPL). The active target region lies within the range $-5.5 < z < 0$. cm.

3.4 Charged particle analysis

Analysis of secondary charged particles, which for the most part are produced within the target, consists of three correlated tasks: tracking, momentum measurement, and identification. The detector components described in this section are designed to

⁸At E769’s center-of-mass energy, $\sigma_I(pp) \simeq \sigma_I(pn) \simeq 33$ mb, while $\sigma_I(\pi N) \simeq \sigma_I(KN) \simeq 20$ mb.

provide the information used in the reconstruction of charged particle 4-momenta, a process described in Chapter 5.

3.4.1 Silicon microstrip detector

High-resolution tracking of charged particles, allowing for separation of production and decay vertices for charm meson species, is made possible through the use of a silicon microstrip detector (SMD), located immediately downstream of the interaction scintillator ($0.2 < z < 23.9$ cm). The SMD consists of eleven 300μ thick silicon planes, each of whose upstream (downstream) surfaces have been imbedded with B (As) atoms to form a p(n)-type semiconductor layer. The diffusion of holes (electrons) from the p(n)-type surfaces into the Si inner region creates an electric field directed toward the upstream surface; this field is strengthened by the application of an external voltage (70-90 V). When a charged particle passes through the plane, the resulting ionization creates electron-hole pairs; the electric field sweeps the electrons (holes) to the n(p)-type surface. This voltage signal is picked up by the nearest member of a parallel array of instrumented Al electrodes deposited onto the upstream surface at a pitch of 50μ (25μ for the two most upstream planes). Each SMD plane therefore measures the transverse location of the charged particle in the direction perpendicular to the orientation of the Al microstrips. Of the eleven planes, 4 are x -view, 4 are y -view, and the remaining 3 are v -view, where the v -axis is formed by a right-handed rotation of the x -axis by 20.5° in the transverse plane. The number of instrumented channels on each plane ranges from 300 to 1000.

The 25 (50) μ planes have typical efficiencies of 70% (92%) and resolutions of 16 (21) μ ; these resolutions can be compared with the RMS deviation of a flat distribution with the appropriate pitch width: 7 (14) μ . As a whole, the SMD system provides vertex resolution of $\sim 15 \mu$ in the transverse plane; vertex resolution in z is on the order of hundreds of microns. The charged track multiplicity of a typical event is 10-15, resulting in SMD channel occupancies on order of a few percent.

3.4.2 Drift chambers

Downstream of the SMD system, four sets (D1-D4) of drift chambers (DC), interspersed among two analysis magnets (M1 and M2), are used for momentum and charge sign measurement of charged particles. Each of the sets consist of 1-4 assemblies; each assembly contains a set of 3-4 sense wire planes bathed in a 1:1 Ar-ethane gas mixture. Alternating with the sense wire planes are HV cathode planes formed by parallel wires held at a voltage of -2400 V. Each sense wire plane is made up of alternating sense and field-shaping wires; the former are grounded while the latter are held at -2000 V. The resulting field configuration is designed so that free electrons drift with uniform speed towards the nearest sense wire. When a charged particle passes through the DC gas, ionization occurs. Acceleration of these liberated electrons into other gas molecules causes secondary ionization, increasing the voltage signal received when the electrons reach the sense wire. The constant drift velocity allows the use of timing information in improving the spatial resolution beyond that obtainable on the basis of sense wire pitch alone; a two-fold degeneracy in this measurement results, however, from not knowing the direction from which the electrons drifted.

DC set	number of assemblies	pitch (cm)	active area (m ²)	average z position (m)	views per assembly
D1	2	0.5	0.91	1.75	uvx'
D2	4	0.9	3.9	4.43	uxv
D3	4	1.5	4.6	9.89	uxv
D4	1	3.0	13.3	17.45	uxv

Table 3.3: DC parameters.

Each plane measures a transverse coordinate in one of four views: x , x' , u , or v . The sense wires of x and x' -view planes are in alternating positions, thereby alleviating the measurement degeneracy in that dimension; the u and v views measure positions along axes obtained by a 20.5° right(left)-handed rotation of the x -axis. Important DC parameters for the four sets are given in Table 3.3. As shown in Fig. 3.1, the

DC sets are located (D1) between the SMD and M1, (D2) between M1 and the first Čerenkov counter (C1), (D3) between M2 and the second Čerenkov counter (C2), and (D4) between C2 and the calorimeters.⁹ DC tracking is supplemented by two y -view PWC planes of 0.2 cm pitch, which are interspersed with the D1 assemblies. The operating principle behind a PWC is similar to that of a DC; for the former, however, timing information is not used to improve the spatial resolution beyond that determined by wire pitch.

Plane efficiencies for the DC system range from 68-92%; resolutions on the order of a few hundred microns are typical. Each DC plane has a central region of reduced efficiency due to the high passage rate of particles near the beam line; the shapes of these “holes” are measured and parametrized for each assembly so that this effect may be incorporated into the MC simulation of the spectrometer (see Section 4.2).

3.4.3 Magnets

Momentum analysis of charged particles consists of tracking their trajectories into and out of a known magnetic field (and correctly matching the two track segments). The angular deflection of the track (as measured by DC tracking) and the p_T “kick” given to a relativistic charged particle passing through the magnet determine the particle’s momentum. Parameters for E769’s two analysis magnets (M1 and M2) are given in Table 3.4. The fields of these magnets are oriented along the y -axis.

For charged tracks passing through M1 and M2, the fractional momentum resolution is given by

$$\frac{\delta p}{p} = \sqrt{(0.1\%/GeV \times p)^2 + (0.5\%)^2}, \quad (3.3)$$

where the second term arises from multiple scattering.

⁹Tracks are conceptually divided into four categories, depending on which DC sets they traverse. These categories are labelled by the variable JCATSG, which takes on values 1, 3, 7, or 15 for tracks which penetrate past D1, D2, D3, and D4, respectively. This analysis uses only JCATSG ≥ 3 tracks, i.e., tracks which have passed at least through M1.

Magnet	M1	M2
entrance aperture (cm ²)	154 × 73	154 × 69
exit aperture (cm ²)	183 × 91	183 × 86
geometrical acceptance (mrad ²)	±240 × ±120	±120 × ±60
z length (m)	1.65	2.08
current (kA)	2.5	1.8
p_T kick (GeV)	0.21	0.32

Table 3.4: Magnet parameters.

3.4.4 Čerenkov counters

E769's two threshold Čerenkov counters (C1 and C2) are located just downstream of D2 and D3, respectively. Unlike the DISC, which identifies a beam particle of known trajectory by detecting Čerenkov light emitted at a fixed angle, the downstream detectors are designed to identify multiple charged tracks passing through their respective gaseous medium at various angles and at the same time. As discussed in Section 3.2, Čerenkov light is emitted when the speed of a charged particle in a medium exceeds the speed of light in that medium, given by c/n , where c is the speed of light in vacuum and n is the index of refraction of the medium. This threshold for Čerenkov radiation can be rewritten in terms of the mass and momentum of the particle:

$$\frac{p}{m} > \sqrt{n^2 - 1}. \quad (3.4)$$

From this relation it is clear that, for a given n , charged particles emit Čerenkov light above a momentum threshold proportional to their mass. By correlating the responses of two detectors filled with gases of different n to a given particle of known momentum, discrimination between π , K , and p is possible in a momentum range bounded by the lower π and higher p thresholds. C1 (C2) is filled with N₂ (80% N₂, 20% He) gas, which at operating density has an n value of 1.000350 (1.000088). The logical states of the two detectors are given in Table 3.5.

Momentum range (GeV)	π	K	p
0 - 6	(0,0)	(0,0)	(0,0)
6 - 9	(1,0)	(0,0)	(0,0)
9 - 20	(1,1)	(0,0)	(0,0)
20 - 36	(1,1)	(1,0)	(0,0)
36 - 38	(1,1)	(1,1)	(0,0)
38 - 69	(1,1)	(1,1)	(1,0)
> 69	(1,1)	(1,1)	(1,1)

Table 3.5: (C1,C2) logical states. 1 = on, 0 = off.

At the downstream end of each counter, a segmented mirror, designed to minimize the overlap in a single mirror of Čerenkov photons from separate particles, allows for simultaneous identification of multiple particles. The reflected light from each mirror is focussed by a conical light guide for collection by a particular PMT. In this analysis, C1 and C2 information is used only to exclude identified pions as candidate kaons. See Section 7.2.2 for a discussion of the kaon identification efficiency achieved by the Čerenkov counter pair.

3.5 Triggers

During the E769 running, beam particles impinged upon the target at a rate of ~ 1 MHz. Given the 2.5% interaction length target, physics events of some kind are expected to occur at a rate on the order of 25 kHz. The E769 data acquisition (DA) system¹⁰ can only write events to tape at 450 Hz, thus requiring a rejection factor of roughly 50 be applied to interaction events; this is the job of the E769 triggers. Fast on-line electronics convert various experimental analog signals into binary logical signals (bits); event triggering is implemented by inputting these as well as other user-defined bits (e.g., prescalers) into a programmable logic unit (PLU), which outputs

¹⁰Detailed descriptions of the E769 DA system can be found in the references listed in [40].

for each trigger type a binary signal defined as a logical operation on some number of input bits. One PLU input bit which is included in the logical definitions of all trigger types is the strobe signal; this indicates that the DA system is not currently busy with another event. Output of a PLU trigger bit signals the DA system to write the current event to tape; the logical states of all PLU input and output bits are included as data words in the event, allowing for off-line identification of the trigger type(s) under which it was written to tape.

The most basic trigger type is the interaction trigger, which indicates that a beam particle has entered the target and that an inelastic interaction has occurred. Specifically, coincident signals¹¹ are required from the two TRD beam scintillators, the beam counter, and the interaction scintillator. This last signal must exceed a threshold corresponding to the passage of more than five minimum-ionizing charged particles. In addition, a signal from the beam halo counter acts as a veto. In and of themselves, interaction trigger events are not particularly interesting for purposes of studying charm; as described in Section 7.2.1, however, the efficiency of each combination of trigger types used in this analysis is measured with respect to that of the (unprescaled) interaction trigger. Therefore, this trigger is written to tape, but is prescaled by a factor ranging from 100-600; interaction triggers make up about 5% of the data set. Note that the input bit combination defining the interaction trigger (excepting its prescaler) is required in the logical definitions of all other trigger types as well.

By comparing the cross-section predicted for $c\bar{c}$ production with that measured for all inelastic collisions, we see that less than 0.1% of interaction trigger events are expected to contain charm. E769 makes use of transverse energy (E_T) triggers to enhance the charm content of the data set written to tape. Although calorimeter information is not directly used in this analysis, it provides the means of triggering on events with E_T above a desired threshold. We therefore give a brief description of the calorimeters before proceeding to define the different trigger types.

E769's calorimeters are located downstream of D4. Electromagnetic calorimetry

¹¹Logical simultaneity is achieved by delaying signals by amounts given by their relative positions and proximities to the electronics.

is provided by the segmented liquid ionization calorimeter (SLIC), which consists of 60 alternating layers of lead absorbers and liquid scintillator, comprising 20 radiation lengths. The scintillating liquid is confined to corrugations of a teflon-coated aluminum sheet bent into a square wave; these corrugations form light guides leading to PMT channels. Each scintillator layer therefore allows characterization of an electromagnetic shower in the u , v , or y -view, as previously defined. The pitch of the detector is given by the half wavelength of the Al square wave, 3.17 cm. Behind the SLIC is the hadrometer, a 6-absorption-length hadronic calorimeter made up of 36 alternating layers of steel absorbers and plastic scintillator. The plastic scintillator is apportioned into 14.5 cm wide strips, leading to PMT channels and providing energy deposition measurements in the x and y -views.

The quantity E_T is a weighted sum of energy deposited in the calorimeter channels, where the weighting factor is the distance from a given channel to the beam line. This summation takes place over a 200 ns window, corresponding to about 10 buckets. Events whose E_T exceeds a threshold of about 5.5 GeV turn on the ETin bit; a higher threshold (~ 8 GeV) defines the EThigh bit.¹² Additional physical PLU input bits include the occurrence of a DISC signal (satisfying the requirements detailed in Section 3.2) and the measurement of an energy deposit of $E_T > 0.5$ GeV in a single SLIC y -view channel (ELEC), signaling the presence of a high- p_T electron. During most of the positive running, the \overline{KB} bit is used to disallow events followed closely (within 150 ns) by another beam particle; this lessens the contamination of E_T by energy from neighboring “out-of-time” events. The logical definitions of the trigger types used in this analysis are given in Table 3.6. Note that prescaler settings varied during the running, ranging from 5-60 (1.5-100) for $ET\pi$ (ETB).

As detailed in Section 6.2, various combinations of these trigger types characterize events making up the data subsets used in this analysis. The efficiencies of these trigger combinations are given in Section 7.2.1. The efficacy of E_T triggering for charm is evidenced by difference in the typical ETin bit efficiency for charm and generic interaction events: 80% and 25%, respectively. In the negative (positive) running, ETK triggers are used to enhance the fraction of events caused by interactions of

¹²These thresholds were subject to some variation during the E769 running.

Trigger type	PLU input bits
ET π	ETin · PS ₁ · KB ^a
ETB	EThigh · PS ₂ · KB ^a
ETK	ETin · DISC
ETe	EThigh · ELEC · KB ^a

^aThe \overline{KB} bit was operative only during the positive running.

Table 3.6: Logical definitions of trigger types.

kaon (kaon or proton) beam particles with the target.

3.6 Scalers

In order to provide an absolute normalization for the forward cross-section calculations, the number of beam particles incident on the target must be counted. In addition, running tallies of various experimental quantities provide valuable diagnostic information during both the running (as witnessed by the name “counting room”) and analysis phases¹³ of the experiment. For these purposes, E769 implemented a multitude of scalars into the electronic logic of the DA system. In this section, we discuss only those used in this analysis.

The “good beam” scaler N_{BEAM} takes as its input the same signals as the interaction trigger, with the exception of that from the interaction scintillator. In other words, N_{BEAM} counts the number of beam particles impinging of the target; the veto provided by the beam halo counter insures that the beam particle actually hits the target. Another important beam scaler is N_{DISC} , which counts the number of four-fold coincidences in the DISC (with at least one hit in each quadrant). The role of each of these scalars in the forward cross-section calculations is detailed in Section 8.1.

The average fraction of time that the DA system is available for event writing

¹³For example, nonsensical values of certain scaler ratios recorded in a particular spill are used to throw out that spill as “bad” in the off-line event weeding process, discussed in Section 6.1.

is known as the detector livetime ϵ_{live} ; this quantity figures directly in the cross-section formula. The livetime is calculated as a ratio of scalers, specifically the ratio of the scaler downstream of the PLU counting prescaled interaction triggers to the corresponding upstream scaler. Since the PLU is disabled while the DA system is busy with an event, this ratio provides a direct measure of ϵ_{live} . Values of $\sim 75\%$ for ϵ_{live} are typical.